JOURNAL OF COMPUTATIONAL PHYSICS 6, 392–405 (1970)

Conservation Properties of Convection Difference Schemes

STEVE A. PIACSEK* AND GARETH P. WILLIAMS

Geophysical Fluid Dynamics Laboratory/NOAA, Princeton University, P. O. Box 308, Princeton, N. J. 08540

Received May 8, 1970

The so-called conservative or flux form of the finite difference formulation of convection terms is shown to be inadequate for preventing nonlinear instability in some cases. A preferred scheme for the convection terms which has the property of *absolute* spatial conservation is obtained. Illustrative examples are given for (i) the Navier–Stokes equations; (ii) a forced convection equation; and (iii) a Burger's type equation.

1. INTRODUCTION

Early investigations of long-term time integrations involving nonlinear convection terms revealed the presence of a weak instability that eventually led to meaningless results. The instability could not be cured by shortening the time step. This so-called nonlinear instability was shown by Phillips [1] to be due to aliasing. Arakawa [2] then proved that it is possible to devise forms of the discrete convection terms with which the instability does not occur because the aliasing is controlled. The principle is that stability can be maintained if the discrete convection form is designed so that the integral of the quadratic quantity is conserved (in addition to the usual Courant–Friedrichs–Lewy linearized stability condition on the time step Δt). As nonlinear instability is due to spatial truncation rather than to time truncation, our discussion and use of the term "conservation" will refer in the main to the spatial aspect of the integration.

Quadratic conserving forms of the convection terms were given by Arakawa [2] for the two-dimensional vorticity equation and by Lilly [3] and Bryan [4] for the general primitive form of the hydrodynamic equations. In each of these schemes the conservation of quadratic quantities depends on the divergence $\mathscr{D} \equiv \nabla \cdot \mathbf{v}$ being identically zero at all stages of the calculation. In some methods of integration continuity is identically satisfied through the use of a stream function. However, in the primitive equation forms used in the integration methods of, e.g., Harlow

* Now at the Applied Mathematics Division, Argonne National Laboratory, Argonne, Ill.

and Welch [5] and Williams [6], continuity is not identically satisfied but is maintained at a small value $\mathscr{D}$, the precise value of which depends on the accuracy to which the associated Poisson equation for pressure is solved. Because of this nonvanishing value of $\mathscr{D}$ it is necessary to re-examine the derivation of the discrete convection schemes.

The difference scheme derived will be applicable, in addition to the Navier–Stokes equations, to other transport equations with convection terms present. Such equations are the induction equations of magnetohydrodynamics, the transport of "active scalars" such as heat, mass, or solutes in liquids that can influence the motion and the transport of "passive scalars" such as tracers and pollutants in atmospheric and oceanic flows.

2. The Finite Difference Equations

Numerical methods for integrating equations involving convection terms are in general use. It will be convenient to refer to a typical method, that discussed by Williams [6]. In that study the convection terms were written in the standard flux form, shown by Bryan [4] to be conserving of quadratic quantities. However, it has become apparent that such discrete convection terms do not conserve quadratic quantities absolutely, i.e., algebraically. This flux form is not fully adequate for prediction methods which involve a process in which the continuity variable $\mathscr{D} = \nabla \cdot \mathbf{v}$ is not identically zero. The nonvanishing of $\mathscr{D}$ limits the validity of Bryan's analysis for this method.

To illustrate the problem, consider a typical transport equation such as that for heat in an adiabatic fluid,

$$\frac{\partial T}{\partial t} + (\mathbf{v} \cdot \nabla)\, T = 0. \tag{1}$$

For a term such as wT_z the finite difference expression in standard flux form is

$$C_1(w, T) \equiv \delta_z(w\bar{T}^z), \tag{2}$$

where we define the central difference operators

$$\delta_z T \equiv \left[T\left(z + \frac{\Delta z}{2}\right) - T\left(z - \frac{\Delta z}{2}\right)\right]\Big/\Delta z, \tag{3}$$

$$\bar{T}^z \equiv \left[T\left(z + \frac{\Delta z}{2}\right) + T\left(z - \frac{\Delta z}{2}\right)\right]\Big/2, \tag{4}$$

for the grid system of Fig. 1. Δz is the distance between adjacent T points. (See

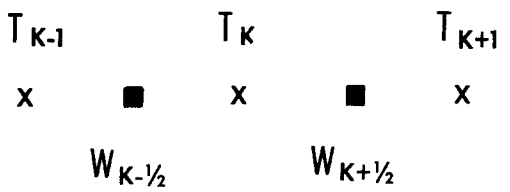

FIG. 1. The grid point arrangement.

Williams, Ref. [6], for full details of grid arrangement and boundaries for the Navier–Stokes equations.) Upon forming the corresponding temperature variance equation the term of Eq. (2) produces a contribution

$$T\,\delta_z(w\bar{T}^z) = \delta_z\left(w\,\frac{\widetilde{TT}^z}{2}\right) + \frac{T^2}{2}\,\delta_z\,w, \tag{5}$$

where we define

$$\widetilde{TT}^z \equiv T\left(z+\frac{\Delta z}{2}\right)\cdot T\left(z-\frac{\Delta z}{2}\right). \tag{6}$$

The first term on the right side of (5) is in the correct form for the conservation of T^2. However, the vanishing of the second term, when contributions from the other convection components are considered, will depend on the satisfaction of local continuity, $\mathscr{D} = 0$. In certain numerical schemes such as those Bryan [4] had in mind local continuity is achieved and there is no problem. But in methods such as that of Harlow and Welch [5] and Williams [6] $\mathscr{D}$ is a nonvanishing small quantity. Thus a summation of terms such as (5) over the whole fluid gives a nonvanishing contribution

$$+\Sigma\,\frac{T^2}{2}\,\mathscr{D}. \tag{7}$$

This term (and its equivalent in the momentum transport equations, etc.) reduces the accuracy of the conservation of quadratic quantities and hence the stability of the form C_1. The conservation by the form C_1 is dependent upon the value of $\mathscr{D}$ and will therefore be referred to as a *conditionally conserving* form. Although the term (7) appears small it can cause critical problems in computations with null or small diffusive terms, as the examples will show. Clearly the problem is best avoided by using a difference scheme for the convection that does not have conditional conservation. In methods where the Poisson equation is solved by a relaxation process the residual $\mathscr{D}$ is much larger and problems are accentuated.

To obtain a convection scheme which has no $\mathscr{D}$ contribution, we consider a second form

$$C_2(w, T) \equiv \overline{w\delta_z T}^z, \tag{8}$$

which is related to the first by the identity

$$\overline{w\delta_z T}^z = \delta_z(w\bar{T}^z) - T\delta_z w. \tag{9}$$

The C_2 form produces a contribution

$$-\Sigma \frac{T^2}{2}\mathscr{D} \tag{10}$$

to the temperature variance integral so that by averaging the two forms C_1 and C_2, the $\mathscr{D}$ contributions to the variance equation can be made to cancel and we obtain a form C_3 which is *absolutely conserving*, i.e., the conservation is algebraic and is independent of the accuracy of the solution. This form is written

$$C_3(w, T) \equiv [\delta_z(w\bar{T}^z) + \overline{w\delta_z T}^z]/2, \tag{11}$$

and it has a simple fundamental form when expressed for the grid arrangement of Fig. 1. The form is

$$C_3(w, T)_k = [w_{k+1/2}T_{k+1} - w_{k-1/2}T_{k-1}]/2\Delta z. \tag{12}$$

It should be mentioned that the form C_3 has the disadvantage of introducing errors proportional to $\mathscr{D}$ into the integrals of linear quantities. However, linear conservation is not as meaningful or as necessary a requirement for computational stability as quadratic conservation. Hence it is recommended that the form C_3 be used both to avoid possible difficulties from arising and to reduce computational time, since the expression (12) for C_3 involves less calculation than that for C_1 or C_2.

3. Illustrative Solutions

In this section we present solutions obtained for three different problems involving convection terms. The differences between solutions using the C_1 and C_3 discrete convection schemes will be examined in each case. Each example indicates how the schemes behave for different types of convection.

Only time integration schemes that are essentially nondamping have been considered, i.e., for which linearized stability analysis shows the associated eigenvalues to lie on the unit circle. The methods of Lax–Wendroff [7] and Leith [8], and the

ADI method of Douglas [9] in the nonlinear case, were found unacceptable for this reason. The commonly known "leap-frog" method [10] and the lesser known "angled-derivative" method [11] were found satisfactory for the purpose of this study.

3.1. *Example* 1. *The Navier–Stokes Equations*

Solutions were obtained for an inviscid flow by the method given by Williams [6] for solving the Navier–Stokes equations. Setting the viscosity to zero places the severest test on the numerical formulation and most clearly shows the differences between the conditional and absolute conserving schemes.

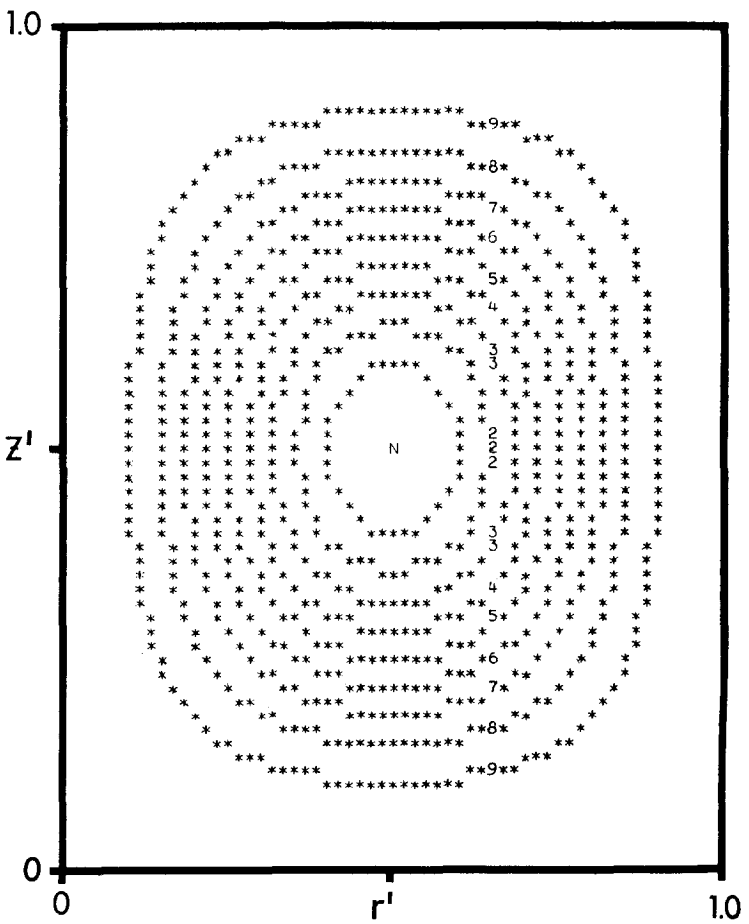

FIG. 2. Initial stream function of Example 1.

As an example, we consider the evolution of a cellular flow in an annular gap. The flow is assumed to be inviscid and barotropic so that there is no external source of energy. Thus the initially imposed kinetic energy should remain constant. How well this condition is met by each computational scheme will be a measure of that scheme's behavior. Since the flow is assumed to be axially symmetric, the governing equations are

$$\delta_t \bar{v}^t + C(\mathbf{v}, v) = -\delta_r \pi, \tag{13}$$

$$\delta_t \bar{w}^t + C(\mathbf{v}, w) = -\delta_z \pi, \tag{14}$$

$$\mathscr{D} \equiv \frac{1}{r}\,\delta_r(rv) + \delta_z w = 0, \tag{15}$$

where v, w, π are the radial velocity, vertical velocity, and pressure, respectively. The equations are solved by marching with centered time differences and using the continuity equation (15) to give a Poisson equation for the pressure. The full details of the grid and boundary arrangement are in the paper by Williams, Ref. [6]. The fluid is given initial kinetic energy by specifying a cellular motion, Fig. 2, in the r, z plane in terms of normalized coordinates r', z',

$$\psi = -3 \sin^2 \pi z' \cdot \sin^2 \pi r', \tag{16}$$

$$rv = -\delta_z \psi, \qquad rw = +\delta_r \psi, \tag{17}$$

with zero normal velocities at all boundaries. The convection schemes in axially symmetric cylindrical polar coordinates are

$$C_1(\mathbf{v}, v) \equiv \frac{1}{r}\,\delta_r(\overline{rv}^r \cdot \bar{v}^r) + \delta_z(\bar{w}^r \bar{v}^z), \tag{18}$$

$$C_1(\mathbf{v}, w) \equiv \frac{1}{r}\,\delta_r(\overline{rv}^z \cdot \bar{w}^r) + \delta_z(\bar{w}^z \bar{w}^z), \tag{19}$$

$$C_2(\mathbf{v}, v) \equiv \frac{1}{r}\,\overline{(\overline{rv}^r \delta_r v)}^r + \overline{(\bar{w}^r \delta_z v)}^z, \tag{20}$$

$$C_2(\mathbf{v}, w) \equiv \frac{1}{r}\,\overline{(\overline{rv}^z \delta_r w)}^r + \overline{(\bar{w}^z \delta_z w)}^z. \tag{21}$$

The averaging in the C_1 forms is necessitated by the staggered grid and this

particular form is chosen as it provides quadratic conservation. The C_2 forms are derived from the C_1 forms by use of the identity (9). The kinetic energy K is defined as the summation of

$$\frac{1}{2}\left(\overline{w^2}^z + \frac{1}{r}\overline{rv^2}^r\right) \tag{22}$$

over all fluid elements centered on the pressure point. The C_3 forms are given by averaging the corresponding C_1, C_2 terms.

Other parameters of the calculation are (i) the interior radius, $a = 2$ cm; (ii) the outer radius, $b = 5$ cm; (iii) the depth of the fluid, $d = 3$ cm. A moderate resolution of 20×20 grid lengths was used. The accuracy of the solutions can be improved by increasing the resolution but our purpose is to display the behavior at a given resolution.

TABLE I

Total Change in Kinetic Energy for Both Schemes After 50 sec Computed at Three Values of Δt. Initial Kinetic Energy = 4.8882 cgs units.

Scheme	$10{,}000 \times (\Delta t = 0.005)$	$5000 \times (\Delta t = 0.010)$	$1000 \times (\Delta t = 0.050)$
C_3	−0.0054	−0.0101	−0.0295
C_1	+0.1831	+0.1535	+0.1712

TABLE II

Variation in kinetic energy for both schemes for $\Delta t = 0.005$ over 20,000 steps. Also shown are individual energy components. Initial kinetic energy = 4.8882 cgs units.

Time step	Time in sec	$\Sigma\frac{1}{2}v^2$ with C_3	$\Sigma\frac{1}{2}w^2$ with C_3	ΔK with C_3	ΔK with C_1
0	0	2.3959	2.4923	−0.0000	+0.0000
2000	10	2.8964	1.9917	−0.0001	+0.0170
4000	20	1.7546	3.1332	−0.0004	+0.0338
6000	30	2.2437	2.6438	−0.0007	+0.0308
8000	40	2.8802	2.0064	−0.0015	+0.0428
10,000	50	2.2297	2.6532	−0.0054	+0.1831
12,000	60	2.3314	2.5439	−0.0129	+0.4053
14,000	70	2.5376	2.3300	−0.0206	+0.4503
16,000	80	2.4094	2.4523	−0.0265	+0.4694
18,000	90	2.3677	2.4879	−0.0327	+0.4125
20,000	100	2.2832	2.5659	−0.0390	+0.4354

In analyzing the solutions we must first find out how the time truncation of the centered time differencing affects the solutions so that we can isolate the effects of the space truncation errors which are our present concern. To do this solutions were obtained for three values of the time step increment Δt for the two discrete convection forms C_1 and C_3. The results, Table I, show the change in total kinetic energy after 50 secs caused by computational sources. All the Δt values are below the C–F–L linear stability value of 0.15 for this flow. From Table I we conclude that errors in energy conservation in using the C_3 form are due solely to time truncation errors and that these errors can be made as small as desired by decreasing Δt. However, the errors with the C_1 system are effectively independent of Δt and are due to space truncation errors.

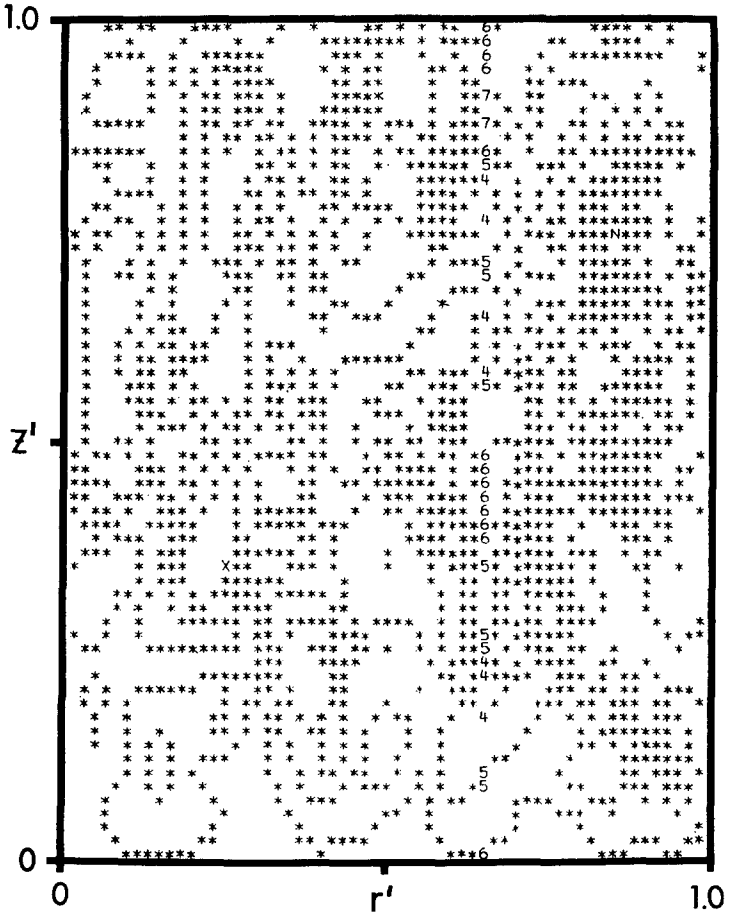

FIG. 3. Final stream function of Example 1.

Next, using the smallest Δt to minimize time truncation effects, we look at solutions over a large number of steps, Table II. The two components of K show that the flow is changing even though the total K remains almost constant. The column for C_3 shows that the time truncation effects are small and that the use of C_1 leads to space truncation errors of an undesirable level. Obviously C_3 is a preferable scheme under the conditions of these solutions. Figure 3 shows the state of the stream function at the end of the calculation.

To estimate under what circumstances the errors caused by using the C_1 form are important, consider the kinetic energy equation that is normally used in the Boussinesq equations of natural convection, i.e.,

$$\frac{\partial K}{\partial t} = \beta g\langle wT\rangle + \nu\langle \mathbf{v}\cdot\nabla^2\mathbf{v}\rangle - \langle \mathbf{v}\cdot(\mathbf{v}\cdot\nabla\mathbf{v})\rangle - \langle \mathbf{v}\cdot\nabla\pi\rangle. \tag{23}$$

The last two terms are zero for the continuous equations but in the finite difference equations they are only zero if the differencing is designed to make them so. In general the last two terms are insignificant when compared to the first two terms. In the example of Williams [6] using the C_1 form, the values obtained were of the order 10^{-1}, 10^{-1}, 10^{-7}, and 10^{-6} for these terms, respectively. Thus for such calculations there is little difference in using either the C_1 or C_3 forms. However, when the first two energy integrals are small or zero, as is the case in adiabatic, inviscid flow, the significance of the last two terms increases. In the example of this section where ΔK is due solely to the latter terms we find that (i) for C_3, $\langle \mathbf{v}\cdot(\mathbf{v}\cdot\nabla\mathbf{v})\rangle \sim 10^{-8}$, $\langle \mathbf{v}\cdot\nabla\pi\rangle \sim 10^{-8}$, and $\mathscr{D} \sim 10^{-9}$ throughout the calculation but (ii) for C_1 the values of $\langle \mathbf{v}\cdot(\mathbf{v}\cdot\nabla\mathbf{v})\rangle$, $\langle \mathbf{v}\cdot\nabla\pi\rangle$, and $\mathscr{D}$ are 10^{-5}, 10^{-8}, 10^{-9} initially, and after 100 sec they have grown to 10^{-2}, 10^{-8}, 10^{-9}, indicating that there is a weak instability in the C_1 convection term. The instability is not present in the C_3 form and can be suppressed in the C_1 form by the presence of diffusive terms.

In all the solutions discussed above, the Poisson equation was solved accurately to within round-off error. When relaxation procedures are used the above-mentioned problems become more acute.

3.2. *Example* 2. *Forced Convection of a Scalar*

The purpose of Examples 2 and 3 is to illustrate the stability of the C_3 difference operator in cases where $\mathscr{D}$ may not be small and where no attempt is made to eliminate or control it as the integration proceeds. Similar to the studies by Roberts and Weiss [11] and Crowley [12], we will first consider a typical forced convection equation, in particular, adiabatic heat flow. For a prescribed velocity field this becomes a linear, variable coefficient, partial differential equation for T,

$$\frac{\partial T}{\partial t} = -\bar{u}(x, z)\cdot\frac{\partial T}{\partial x} - \bar{w}(x, z)\cdot\frac{\partial T}{\partial z} \tag{24}$$

where

$$\begin{aligned} \bar{u}(x, z) &= \sin^2 \pi x \cdot \sin 2\pi z + r_1(x, z), \\ \bar{w}(x, z) &= -\sin 2\pi x \cdot \sin^2 \pi z + r_2(x, z), \end{aligned} \tag{25}$$

and the bar indicates that the velocity field is kept constant during the time integration. The functions r_1, r_2 represent random components whose mean divergence $\bar{\mathscr{D}} \sim 10^{-2}$ on a 40×40 mesh. The sinusoidal components, though satisfying $\nabla \cdot \mathbf{v} \equiv 0$ exactly in their continuous form, fail to satisfy it upon finite differencing by errors $\sim 10^{-7}$. Situations in which such calculations are useful occur commonly in meteorology and astrophysics, where the passive advection of tracers and pollutants in the atmosphere, or of magnetic fields in stars, by an experimentally observed velocity field needs to be investigated over long times.

With the help of (11), Eq. (24) may be written

$$\frac{\partial T}{\partial t} = -C_3(\bar{u}, T) - C_3(\bar{w}, T), \tag{26}$$

and has been integrated on the unit square $0 \leqslant x \leqslant 1$, $0 \leqslant z \leqslant 1$ covered by a 40×40 mesh of grid points. Two different time iteration methods have been applied to (26). These are:

a. The "leap-frog" method (Richtmyer, Ref. [10], p. 17), which has a time truncation error of $O(\Delta t^2)$ and a Von Neumann condition of

$$\Delta t \leqslant \Delta x \Big/ \left(| u | + \frac{\Delta x}{\Delta z} | w | \right)$$

associated with it,

$$\frac{1}{2\Delta t} (T_{ij}^{\tau+1} - T_{ij}^{\tau-1}) = -C_3(\bar{u}, T^{\tau}) - C_3(\bar{w}, T^{\tau}). \tag{27}$$

b. The two-sweep "angled-derivative" method (Roberts and Weiss, Ref. [11], p. 279) which has a time truncation error of $O(\Delta t^2/\Delta x^2)$ and no time step limitation associated with it.

Upsweep ($j = 1, 2, \ldots, J$; $i = 1, 2, \ldots, I$),

$$\frac{T_{ij}^{\tau+1} - T_{ij}^{\tau}}{\Delta t} = -C_3^{-}(\bar{u}, T^{\tau}) - C_3^{-}(\bar{w}, T^{\tau}). \tag{28a}$$

Downsweep ($j = J, J-1, \ldots, 1$; $i = I, I-1, \ldots, 1$),

$$\frac{T_{ij}^{\tau+2} - T_{ij}^{\tau+1}}{\Delta t} = -C_3^{+}(\bar{u}, T^{\tau+1}) - C_3^{+}(\bar{w}, T^{\tau+1}), \tag{28b}$$

where we define

$$C_3^-(\bar{u}, T^\tau) = (\bar{u}_{i+1/2,j}T^\tau_{i+1,j} - \bar{u}_{i-1/2,j}T^{\tau+1}_{i-1,j})/2\Delta x,$$
$$C_3^+(\bar{u}, T^\tau) = (\bar{u}_{i+1/2,j}T^{\tau+1}_{i+1,j} - \bar{u}_{i-1/2,j}T^\tau_{i-1,j})/2\Delta x. \tag{29}$$

Each method of time iteration was repeated with different sizes of the time step Δt (the particular values depending on the stability condition of the method) in order to separate the effects of time truncation errors from that associated with the divergence $\mathscr{D}$ and spatial truncation in general. We must also make a remark concerning the boundary conditions on T. Since (24) is first order in x and z, we may specify T only on two sides of the square, say on $x = 0$ and $z = 0$. However, the nature of the staggered grid (shown in Fig. 1) upon which scheme C_3 is built precludes the use of the boundary values of T, and the calculations effectively use $T = 0$ on the boundaries.

As initial conditions, at $t = 0$, $T(x, z)$ is defined as zero everywhere except on a circle of radius $r = 0.15$ centered at $x = 0.35$, $z = 0.35$ in the unit square. On the circle the values of T describe a cone, i.e.,

$$T(x, z) = A[r^2 - (x - 0.35)^2 - (z - 0.35)^2].$$

Integrations were carried out for $\Delta t = 0.0025$, 0.010, and 0.040, respectively, where the critical Δt_{CR} given by the C–F–L condition is 0.025 (see Table III). At $t_N = 50.0$ the integrations were stopped, with the temperature variance determined by some schemes increasing monotonically and others oscillating about some mean value. It was found best, therefore, to define the following quantities:

$$E(t = 0) = E_0 = \sum_{i,j} T^2_{ij}(t = 0), \qquad \bar{E} = \frac{1}{N}\sum_{n=1}^{N} E(t_n),$$
$$\Delta E = (\bar{E} - E_0)/E_0, \qquad E^* = E(t_N)/E_0, \qquad \delta E = \max | E - E_0 |/E_0 \tag{30}$$

In those cases where the iterations diverged E^* is given, otherwise ΔE and δE are given. To compute δE, the initial peak in the energy *vs* time curve is neglected; in most cases, δE corresponds to the amplitude of quasisinusoidal oscillations in E superposed on $\bar{E}$.

The results showed that in the case r_1 and r_2 are set to zero, the same results are obtained with the C_1 and C_3 schemes to five significant figures. When r_1 and r_2 are nonvanishing, C_1 yields divergent results at t at 35 sec but C_3 remains convergent for all values of $\Delta t \leqslant \Delta t_{CR}$. On a comparison with the results of Example 1, we may conclude that linear systems can remain stable with a much larger value of $\mathscr{D}$ than nonlinear systems. We may note that although linearized stability analysis

TABLE III

Change in Variance $\Sigma_i \Sigma_j T_{ij}^2$ for Both Schemes After 50 sec, at Three Values of Δt and with Two Time Methods when r_1, $r_2 \neq 0$ (ANG = angled-derivative, LF = leap-frog, ΔE, δE, E^* given by (30)).

		$\Delta t = 0.0025$ (20,000 steps)			$\Delta t = 0.010$ (5000 steps)			$\Delta t = 0.040$ (1250 steps)
Time scheme	Space scheme	ΔE	E^*	δE	ΔE	E^*	δE	E^*
ANG	C_1		2.100			2.100		∞
	C_3	0.0013		0.0008	0.0115		0.0052	7×10^5
LF	C_1		1.990			2.230		
	C_3	0.0002		0.0000	0.0027		0.0001	—

predicts stability for the angled-derivative method at $\Delta t = 0.040$ ($1.6 \times \Delta t_{CR}$), a slow instability has increased the energy to very large values and the integration is clearly blowing up. The source of this instability is in the time truncation errors.

3.3. *Example* 3. *Two-Component, Inviscid "Burger's Equation"*

The purpose of this calculation is to illustrate the stability of the C_3 difference operator in highly nonlinear systems in which no restraint is put on $\mathscr{D}$. Consider the case in the calculation of turbulent compressible flows. The system chosen was the following:

$$\frac{\partial u}{\partial t} = -u \frac{\partial u}{\partial x} - w \frac{\partial u}{\partial z}, \tag{31a}$$

$$\frac{\partial w}{\partial t} = -u \frac{\partial w}{\partial x} - w \frac{\partial w}{\partial z}. \tag{31b}$$

Again the initial velocity field is chosen to be that of (25), but now $\mathscr{D}$, originally $\sim 10^{-7}$, will be allowed to vary with time. For boundary conditions we choose the normal velocity to vanish at each wall, which provides the four necessary boundary conditions for (31). The use of the staggered grid will exclude the tangential velocities from entering the calculations.

As in Example 2, a 40×40 mesh is chosen and the staggered grid arrangement of Williams [6] is used for the location of u and w values. The leap-frog and angled-derivative methods were used for the time integration. However, because of the nonlinearities we must further clarify schemes (27) and (28). If in scheme (28) we

TABLE IV

Change in Kinetic Energy for Both Schemes After 25 sec, at Three Values of Δt and with Two Time Methods (ANG = angled-derivative, LF = leap-frog, E^* given by (30)).

		$\Delta t = 0.0005$ (50,000 steps)	$\Delta t = 0.0025$ (10,000 steps)	$\Delta t = 0.0125$ (2000 steps)
Time scheme	Space scheme	E^*	E^*	E^*
ANG	C_3	1.000	1.027	2.42
	C_1	∞	∞	∞
LF	C_3	1.029	1.304	∞
	C_1	∞	∞	∞

replace T by u and w, respectively, and evaluate $\bar{u}$ and $\bar{w}$ (now simply u and w) at time level τ in both (28a) and (28b), we obtain the angled-derivative analog of (31). A similar procedure in (27) will yield the leap-frog analog of (31).

We must note that the system described by (31) permits discontinuities or shocks, but there is no effort made in this paper to study the nature of the solutions, only to show that the C_3 form gives stable numerical solutions even in such cases.

The integrations were carred out to $t_N = 25$ sec, with the results given in Table IV. As in Example 2, E^* respresents the ratio of final to initial energies [see (30)]. All computations with the C_1 difference scheme blew up between $t \simeq 0.5$ and $t \simeq 1.0$ sec. By monitoring the total divergence $\Sigma_i \Sigma_j \mid \nabla \cdot \mathbf{v} \mid_{ij} = \mathscr{D}$ present in the system it was found that the blow-up of the calculations coincided with a sudden large increase in the value of $\mathscr{D}$ by factors of 10^6 or larger. The same increase in $\mathscr{D}$ affected the C_3 integrations only slightly. Part of the divergence increase may be attributed to the formation of discontinuities, a genuine effect of compressibility, but a large part is due to the appearance of random small scale fluctuations which the grid is unable to resolve. The results show that it is possible to maintain computational stability even when the flow becomes physically unrealistic, and care must be taken to interpret the results in such cases.

The effect of the time truncation errors is clearly displayed in the results for the C_3 calculations. With each time method there is an increase in the energy that gets bigger with increasing Δt.

Somewhat surprisingly, the angled-derivative method has proved superior to the leap-frog in this nonlinear problem despite its poor truncation error. Additional tests showed that for $\Delta t = 0.0005$ the energy remained unchanged in the fourth significant figure even after 100,000 steps, showing that it is possible to devise convective difference schemes that conserve in time as well as in space. Admittedly,

one has to pay the price in increased computer time, but with the advent of the "fourth-generation" computers and reduced cost per arithmetic operation, this may not become excessive in the future.

It is interesting to compare the results of Example 1 and Example 3 as displayed in Tables II and IV, respectively. In the former pressure is included and the divergence is controlled by the method of corrective iteration, and the C_3 scheme is slightly damping, whereas the C_1 scheme is amplifying. In the latter case both schemes are amplifying, with the C_1 scheme blowing up in a few hundred time steps.

4. Conclusion

We have shown that quadratic conserving convection schemes can be divided into two classes, those of partial conservation and those of absolute conservation. The absolute conserving form C_3 is found to be preferable because it is both computationally stable under all situations and more economical to compute due to its simpler form.

References

1. N. A. Phillips, An example of non-linear computational instability, "The Atmosphere and Sea in Motion," pp. 501–504, Rockefeller Inst. Press, New York, and Oxford University Press, 1959.
2. A. Arakawa, Computational design for long term numerical integration of the equations of fluid motion. Two-dimensional incompressible flow. Part 1. *J. Comput. Phys.* **1** (1966), 119–143.
3. D. K. Lilly, On the computational stability of numerical solutions of time dependent non-linear geophysical fluid dynamics problems, *Mon. Weather Rev.* **93** (1965), 11–26.
4. K. Bryan, A scheme for numerical integration of the equations of motion on an irregular grid free of non-linear instability, *Mon. Weather Rev.* **94** (1966), 39–40.
5. F. H. Harlow and J. E. Welch, Numerical calculations of time dependent viscous incompressible flow of fluid with free surface, *Phys. Fluids* **8** (1965), 2182–2189.
6. G. P. Williams, Numerical investigation of the three-dimensional Navier–Stokes equations for incompressible flow, *J. Fluid Mech.* **37** (1969), 727–750.
7. P. D. Lax and B. Wendroff, Difference schemes for hyperbolic equations with high order of accuracy, *Comm. Pure Appl. Math.* **17** (1964), 381–398.
8. C. E. Leith, Numerical simulation of the earth's atmosphere, "Methods in Computational Physics," Vol. IV, pp. 1–28, Academic Press, New York, 1965.
9. J. Douglas, Jr., Alternating direction methods for three space variables, *Numer. Math.* **4** (1962), 41–63.
10. R. D. Richtmeyer, "A Survey of Difference Methods for Non-Steady Fluid Dynamics," National Center for Atmospheric Research Technical Note 63-2, 1963.
11. K. V. Roberts and N. O. Weiss, Convective difference schemes, *Math. Comp.* **20**, No. 94 (1966), 272–299.
12. W. P. Crowley, Numerical advection experiments, *Mon. Weather Rev.* **96** (1968), 1–11.